Heliyon 6 (2020) e03714

Contents lists available at ScienceDirect

Heliyon

journal homepage: www.cell.com/heliyon

Research article

Detection of carvacrol in essential oils by electrochemical polymerization

M. Bertuola [a,1], N. Fagali [a], M. Fernández Lorenzo de Mele [a,b,*]

[a] Instituto de Investigaciones Fisicoquímicas Teóricas y Aplicadas (INIFTA, CCT La Plata-CONICET), Facultad de Ciencias Exactas, Departamento de Química, Universidad Nacional de La Plata, Casilla de Correo 16, Sucursal 4, 1900, La Plata, Argentina

[b] Facultad de Ingeniería, Universidad Nacional de La Plata, Calle 47 y 1, 1900, La Plata, Argentina

ARTICLE INFO

Keywords:
Materials chemistry
Electrochemistry
Natural product chemistry
Essential oils
Electrochemical detection
Carvacrol
Thymol
Copper

ABSTRACT

Carvacrol (Carv) and thymol (TOH), components of essential oils, are known by their antimicrobial and antioxidant activity. However, Carv but not TOH seems to be the responsible of anti-inflammatory and inhibition of Cu corrosion properties. Since Carv and TOH are positional isomers, their identification is tricky and GC-MS is usually required. To find simple and inexpensive methods that allow the detection of Carv in presence of TOH (e.g. essential oils), cyclic voltammetry and chronoamperometry tests using Pt and Cu as electrodes in TOH and Carv containing mixtures and essential oils were made. Electrochemical and ATR-FTIR results show that pure phytocompounds and mixtures lead to the formation of polymeric layers on both metallic surfaces. Results show that only Cu is suitable for Carv detection. Potentiostatic and potentiodynamic detection is simple and conclusive in Carv + TOH mixtures and in essential oils due to the formation of a homogeneous blocking Carv electropolymeric layer on Cu.

1. Introduction

Essential oils and their main components have been investigated in the last decades particularly in relation to their anticorrosive, antimicrobial, anti-inflammatory and antioxidant-anticancer activity that were recently reviewed [1, 2, 3]. Moreover, there is a growing interest in exploring their use as nutraceuticals in food matrices due to their physiological benefits. Interestingly, the relationship between polyphenol intake and human health has been investigated and their potential benefits to cardiovascular diseases, hypertension, diabetes, metabolic syndrome, obesity, and cancer was reported [4]. In particular, *Thymus vulgaris* and *Origanum vulgare* were the focus of several studies related to their action against pathogenic bacteria. Phenolic compounds, carvacrol (Carv) and thymol (TOH), their main components, are positional isomers, characterized by their advantageous antimicrobial effects in vivo [5]. The antioxidant properties of Carv have been shown not only *in vitro* but also in animal models of pancreatitis, hepatotoxicity and liver cancer. Possible therapeutic effect of Carv in asthma has also been suggested due to its benefic effects on respiratory symptoms, pulmonary function tests and anti-inflammatory effect [6]. Oregano and thyme essential oils contain Carv and TOH. However, Carv but not TOH, seems to be the responsible of the anti-inflammatory effect of these essential oils [7]. On the other hand, Carv but not TOH, has been proposed as natural inhibitor of the burst release of Cu ions in intrauterine devices as well as an ecological corrosion inhibitor of Cu [8]. Considering that the presence and amount of each isomer in essential oils differs significantly according to the specie of the plant, the time of harvest, part of the plant used, etc., it is crucial to distinguish the presence of Carv from that of TOH when a specific effect assigned to Carv is needed. However, due to their structural similarities, the unambiguous identification is not easy using basic equipment. Consequently, the use of a more complex method such as gaseous chromatography coupled to mass spectrometry (GC-MS) is usually required [9]. This technique was used in this work in order to confirm the presence, identities and relative abundance of each isomer in the oregano and thyme essential oils.

Cyclic voltammetry and chronoamperometry test are proposed here as simple and inexpensive tools to identify Carv and to distinguish it from TOH. Comparison of the sensitivity of Pt and Cu for electrochemical detection throughout electropolymerization of Carv in essential oils was made to select the best option. Pure compounds and three essential oils were used with this purpose: *Origanum vulgare* (high content of Carv, very low percentage of TOH), *Thymus vulgaris* (high content of TOH, low

* Corresponding author.
E-mail addresses: mmele@inifta.unlp.edu.ar, fernandezlorenzom@hotmail.com (M. Fernández Lorenzo de Mele).
[1] Present address: Laboratorio de Biomateriales, Biomecánica y Bioinstrumentación, Escuela de Ciencia y Tecnología, Universidad Nacional de San Martín, 1650 San Martín, Argentina.

https://doi.org/10.1016/j.heliyon.2020.e03714
Received 13 February 2020; Received in revised form 9 March 2020; Accepted 27 March 2020

amount of Carv) and *Origanum x applii* (with a ratio of TOH/Carv close to 6 (50.7%/8.1%)). FTIR analysis of the pure components, essential oils and the electropolymeric layers formed on the electrodes was also included.

2. Materials and methods

Platinum wire (99.7%, Merck, Germany) and cylindrical Cu bar (99.7%, Merck, Germany) with an exposed area of 4.7 cm^2 and 0.626 cm^2 respectively were used as working electrodes for electrochemical experiments, and Pt sheets (99.7%, 1.00 cm^2) and Cu sheets (99.7%, 0.57 cm^2) were used for ATR-FTIR analysis. Pt and Cu electrodes were mechanically polished with emery papers of 1000–2500 grit using water as lubricant, rinsed with ultrapure water and dried with nitrogen. The Pt working electrode was activated in 0.2 M H_2SO_4 by 15 voltamperometric cycles between -0.24 V and 1.40 V at 100 mVs^{-1}.

2.1. Electrochemical assays

Electrochemical assays were performed using a three-electrode cell. A Pt foil was used as counter electrode and a saturated calomel electrode (SCE) as reference electrode. Potentiodynamic steps were perform for Pt from -0.24 V to 1.20 V (5 mVs^{-1}, 4 cycles) in an electrolyte containing 0.2 M H_2SO_4 and 0.01 M of pure phytocompounds (TOH or Carv, Sigma, USA) or 0.35% (v/v) of oregano and thyme essential oils (Laboratorio de Fitoquímica, FCAyF, UNLP, Argentina). Potentiodynamic cycles for Cu electrodes (0.30 V–1.00 V potential range, 50 mVs^{-1} scan rate) and potentiostatic assays at 0.40 V (Carv oxidation peak on Cu) were also included in an alkaline hydroalcoholic electrolyte [10] containing 0.1 M of Carv or TOH and 3.5% (v/v) of each essential oils. Each test was run in triplicate to verify the reproducibility of the data. In all cases, a potentiostat-galvanostat TEQ03 was used and the potential values were referred to the SCE.

2.2. Surface analysis by ATR-FTIR and AFM

ATR-FTIR spectra were obtained in an Agilent Cary 630 spectrometer equipped with an attenuated total reflection Diamond ATR, each spectrum was the result of 256 scans taken with a resolution of 2 cm^{-1}.

Tapping® mode AFM (NanoscopeV; Bruker, Santa Barbara, CA) in topographic mode was used to characterize the substrates, using silicon tips (ArrowTM NCR; NanoWorld, Neuchâtel, Switzerland) (spring constant, 42 N/m; resonance frequency, 285 kHz). Nanoscope 7.30 and Nanoscope Analysis 1.5 softwares were employed to obtain the images (Bruker).

2.3. Gas chromatography–mass spectrometry (GC-MS) analysis

Carv, TOH and essential oils of oregano and thyme were diluted 1/20 with dichloromethane and the injection volume was 1 μl (a split ratio of 50:1). GC-MS analysis was performed using a Perkin Elmer Clarus 500/560D equipment. A capillary column Elite-1MS (30 m × 0.25 mm ID; 0.25 μm, Perkin Elmer) was used. Column temperature was programmed to increase from 60 °C to 180 °C at 3 °C/min rate, then 10 °C/min to 290 °C and isothermal for 3min. Helium gas was used as the carrier at a constant flow rate of 1 ml/min. Injector temperature was set to 230 °C. Chemical compounds identities were determined by comparing their mass fragmentation patterns with those of mass spectra from the NIST database version 2.0.

3. Results and discussion

3.1. Analysis of essential oils composition by GC-MS

The chemical composition of essential oils of *T. vulgaris*, *O. vulgare* y *O. x applii* was analyzed by GC-MS. Results show (Figure 1) that essential oils are mainly rich in phenols (as TOH and Carv) but also contain monoterpene hydrocarbons (as o-cymene, τ-terpinene and β-myrcene), oxygenated monoterpenes (1-terpinen-4-ol, β-linalool and α-terpinenol) and other minority components. The content of the compounds of interest, Carv and TOH, in the essential oils differ markedly. The *T. vulgaris* essential oil contains the highest amount of TOH (78.4%) with low percentage of Carv (2%) while *O. vulgare* has the higher content of Carv (87.6%) with very low amount of TOH (<0.1%). For *O. x applii* essential oil the content of TOH and Carv is 50.7 and 8.1%, repectively. Thus, three natural mixtures with different proportions of Carv and TOH were used to test the efficiency of electrochemical method to detect Carv in presence of its isomer TOH in real samples.

3.2. Electropolymerization of phenolic compounds on Pt electrodes

In order to obtain a simple technique to identify the presence of Carv in essential oils, cyclic potentiodynamic measurements on Pt electrodes were assayed.

3.2.1. Pure carvacrol and thymol

Figure 2 shows the control assay made with Pt (dotted line) in the base electrolyte with the characteristic peaks of H_2 adsorption/desorption at cathodic potentials (E < 0.00 V) and the increase in current density from 0.70 V attributed to the oxidation of Pt with the corresponding reduction at 0.50 V [11].

Figure 2A and B also depict the voltammograms obtained with the addition of 0.01 M Carv and 0.01 M TOH, respectively. If Carv is present (Figure 2A), an anodic peak at 0.87 ± 0.01 V is recorded, showing the oxidation of the phytocompound on Pt surface. Upon increasing the number of cycles, the oxidation peak shifted to more anodic potentials (Table 1) while current decreases continuously. In agreement with previous work, this anodic shift is attributed to the decrease of electron withdrawing groups in the polymer as compared to single molecule of Carv [11]. Interestingly, reduction of oxidized Pt species (PtOx) and H_2 desorption contributions were not present during cathodic scan. A similar behavior was reported for chlorinated phenols on Pt electrodes [11] and can be inferred that the oxidation products of Carv remained on the surface and blocked the active sites hindering the oxidation of Pt and of fresh molecules of Carv from the bulk.

Voltammograms made with TOH solutions (Figure 2B) showed a current peak at 0.82 ± 0.01 V (675 μAcm^{-2}) that decreases upon cycling without shifting the peak potential. The absence of PtOx reduction peak in the voltammograms of both phytocompounds indicates that an irreversible electropolymerization process takes place leading to the deactivation of the adsorption sites [11]. The formation of electropolymeric films would prevent the penetration of phenoxide radicals into the polymer layer, their subsequent oxidation, and the cathodic reduction peak during electropolymerization [11, 12, 13].

3.2.2. Essential oils

To investigate the possibility of detecting Carv between the components of essential oils using cyclic voltammetry with Pt electrodes, three essential oils with different TOH/Carv ratios were assayed. The potentiodynamic record of Pt in presence of *T. vulgaris* essential oil is shown in Figure 2C. Voltammograms are very similar to that recorded with Pt in pure TOH-containing electrolyte (Figure 2B) with an oxidation peak at 0.79 ± 0.01 V that progressively decreases (Table 1) and slightly shifts in the anodic direction. As it was described before, GC-MS analysis of this essential oil showed that TOH was the main component of *T. vulgaris* (78.4%) with a minor content of Carv (2.0%).

When *O. vulgare* essential oil was added to the electrolyte, a broad oxidation peak between 0.67 V and 1.09 V, with a current maximum at 0.86 ± 0.01 V (701 $\mu A/cm^2$) was recorded (Figure 2D). The current density of the anodic peak markedly shifts in the anodic direction in the second cycle (see Table 1). This behavior is similar to that of pure Carv (Figure 2A), the main component of this essential oil (87.6% according to

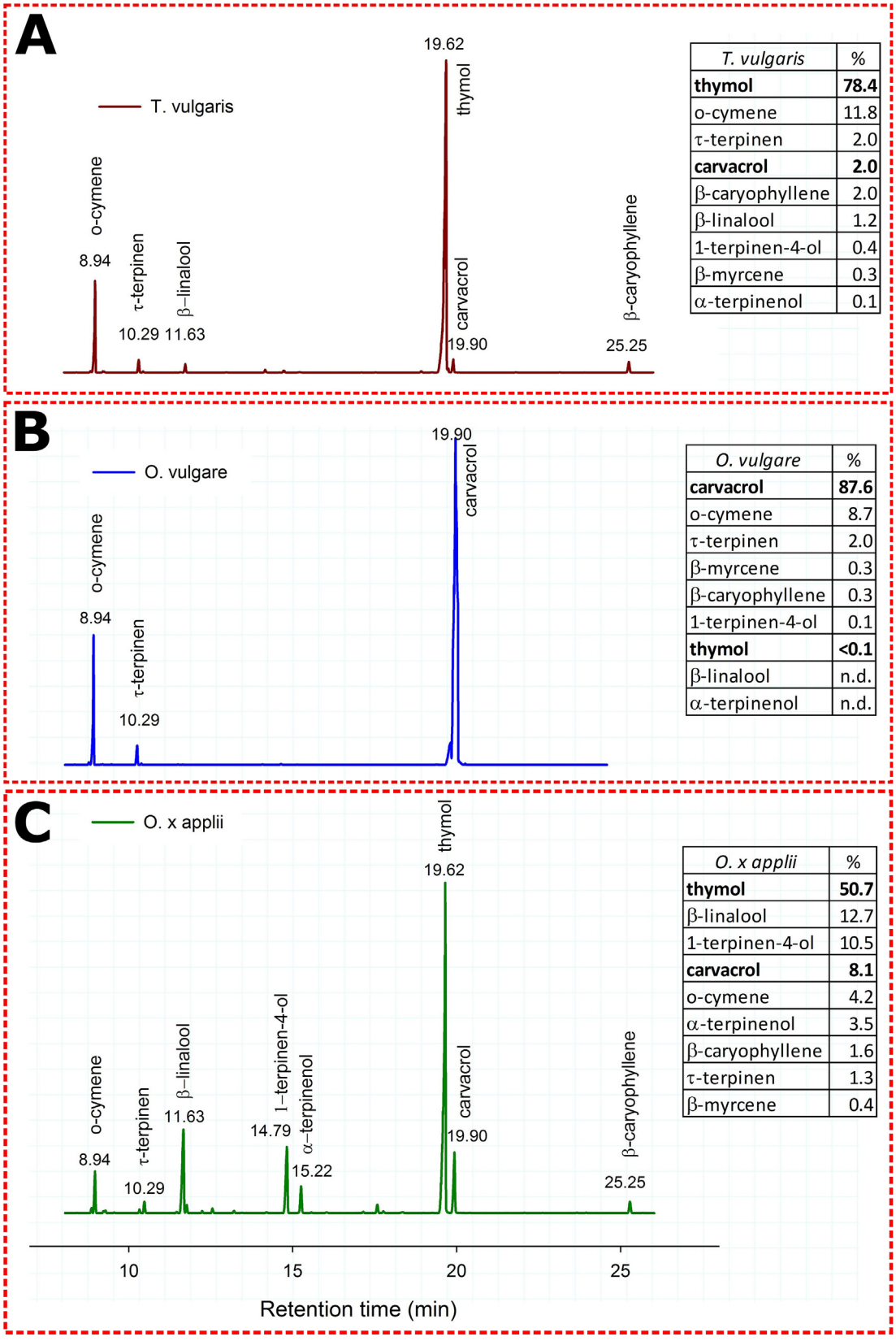

Figure 1. Representative chromatograms of A) *T. vulgaris*, B) *O. vulgare* and C) *O. x applii* essential oils. Identity of each compound was confirmed based on their mass spectra that were compared with NIST database. The tables include the relative amounts of each main compound. The relative content of TOH and Carv were highlighted in bold while the rest of minority compounds were not shown here.

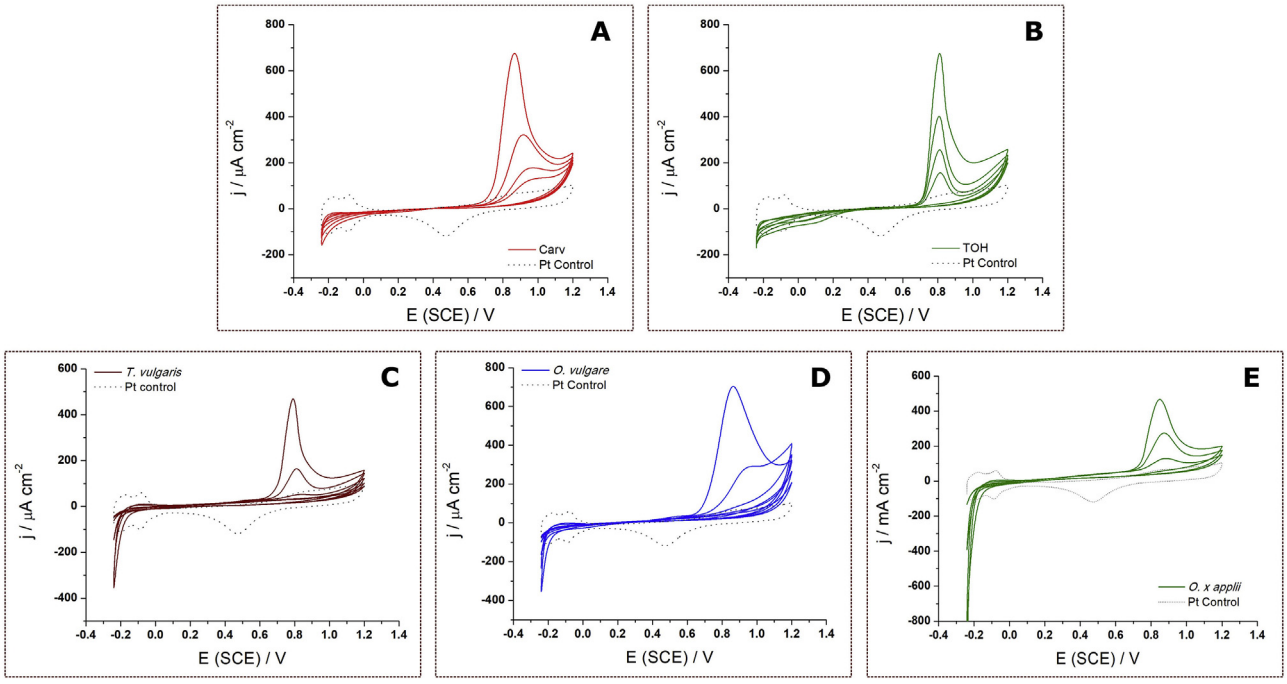

Figure 2. Voltamperometric cycles made at 5 mVs^{-1} with Pt electrodes in 0.2 M H_2SO_4 with: **A)** 0.01 M Carv (red lines), **B)** 0.01 M TOH (green lines). Essential oils in H_2SO_4 electrolyte: **C)** *T. vulgaris* (brown lines), **D)** *O. vulgare* (blue lines) and **E)** *O. x applii* (green lines). Dotted lines represent Pt electrode in electrolyte control without phytocompounds.

Table 1. Oxidation peak potentials (V) obtained from Pt cyclic voltammetry in solutions containing phytocompounds.

Cycles	TOH	Carv	*T. vulgaris*	*O. vulgare*	*O. x applii*
1°	0.82 ± 0.01	0.87 ± 0.01	0.79 ± 0.01	0.86 ± 0.01	0.86 ± 0.02
2°	0.81 ± 0.01	0.92 ± 0.01	0.81 ± 0.01	0.95 ± 0.01	0.89 ± 0.02
3°	0.81 ± 0.01	0.97 ± 0.01	0.84 ± 0.01	0.94 ± 0.02	0.89 ± 0.01
4°	0.81 ± 0.01	0.98 ± 0.01	-	-	-

GC-MS). The amount of TOH in this essential oil is almost undetectable (<0.1%).

Potentiodynamic records in *O. x applii* essential oil are shown in Figure 2E. Again, the decrease in current and the shift in the anodic direction of the potential of the main peak (from 0.86 ± 0.02 V, first cycle, to 0.89 ± 0.01 V in third cycle) can be observed in Table 1. The anodic peak of the voltammogram of this essential oil can be attributed to the presence of TOH, the major component of *O. x applii* (50.7%) that also shows the decrease of the current during cycling. Additionally, a slight shift of the potential of this peak, that resembles that of Carv, could be assigned to the presence of a low but significant content of Carv (8.1%) in the essential oil.

According to these results, *T. vulgaris* essential oil showed voltammograms similar to that of pure TOH (main component) with a peak potential that only slightly shifted during successive cycles. Conversely, voltammograms of *O. vulgare* essential oil, with Carv as main component, resembles that of pure Carv, with an important shift of the peak potential (from 0.87 V to 0.97 V, Table 1) and finally *O. x applii* showed an intermediate behavior with a slight shift of the peak potential (from 0.86 V to 0.89 V). Therefore, the important shift of the peak potential during successive cycles observed in case of *O. vulgare* can be attributed to presence of a high percent of Carv while minor shifts detected for *T. vulgaris* and *O. x applii* are according to the lower amount of Carv and high amounts of TOH in these essential oils. However, differences in the electrochemical behavior using Pt electrodes are not conclusive enough to be used as a method for the detection of Carv when TOH is present.

3.3. ATR-FTIR analysis of pure compounds and the layers formed on Pt electrodes

After observations with naked eye and by optical microscopy it could be noticed that the characteristics of the surface of Pt electrodes after the electrochemical assays changed from brilliant to opaque suggesting the presence of polymer coatings on the Pt surface that seem to be the cause of the decrease in current densities during cycling. To investigate this point ATR-FTIR analysis of the electropolymeric layers were made.

ATR-FTIR spectra of the layers formed on Pt after the electrochemical assays with pure Carv and TOH were compared with those of the essential oils, as shown in Figure 3 and Table 2 and were analyzed in the following sections.

3.3.1. Pure carvacrol and thymol

The infrared spectra of pure Carv and pure TOH (Figure 3A and B, upper panels) show their characteristic contributions. Particularly: v-OH, –OH bend vibration and C–O structures at 3378, 1458, 1251 cm^{-1} (Table 2) that are characteristics of Carv can be noticed and in case of TOH at 3171, 1380 and 1240 cm^{-1}, as can be seen in Figure 3B and Table 2 [14, 15, 16]. Additionally, characteristic signals could be detected for pure Carv, such as 1251 cm^{-1} [15], 1173 cm^{-1} [14,15], 1116 cm^{-1} [14,15], 994 cm^{-1} (1,2,4 substituted phenolic ring) [14, 15], 865 cm^{-1}, 812 cm^{-1} (Carv –CH out of plane vibration) [14, 15] and for pure TOH, e.g. 1286 cm^{-1} [14,15], 1156 cm^{-1} (m-substitution in TOH) [14], 1090 cm^{-1} [14,15], 1041 cm^{-1} (1,3,4 substitution in TOH) [14],

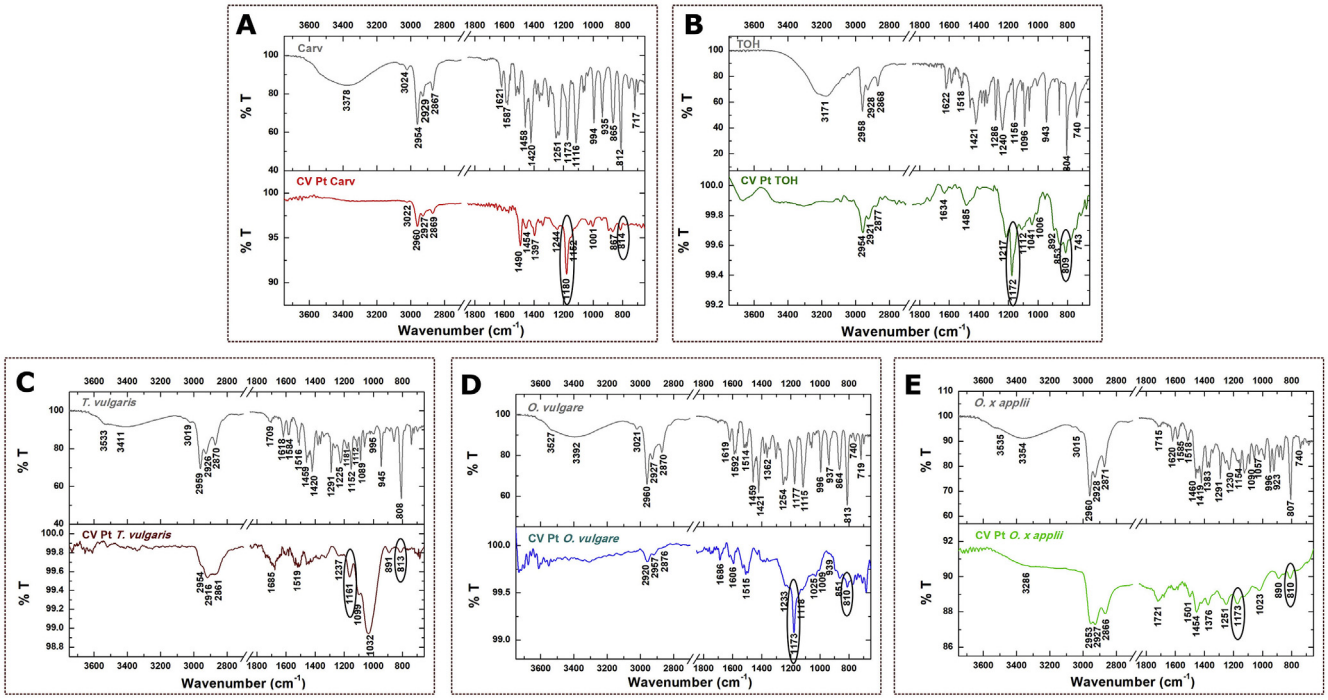

Figure 3. FT-IR spectra corresponding to A) Carv, B) TOH, and the essential oils: C) *T. vulgaris, D) O. vulgare,* E) *O. x applii*. The corresponding spectra obtained for Pt electrodes after the electrochemical assays made with the organic compounds are also included in each case as: A) Pt-Carv, B) Pt-TOH, C) Pt-*T. vulgaris, D)* Pt–*O. vulgare,* E) Pt–*O. x applii.*

Table 2. Wavenumbers and assignments (according to literature data) obtained by ATR-FTIR analysis for pure Carv and TOH and essential oils.

	Carv	TOH	*T. vulgaris*	*O. vulgare*	*O. x applii*
-OH stretching vibration [17]	3378 cm^{-1}	3171 cm^{-1}	3553 and 3411 cm^{-1}	3527 and 3392 cm^{-1}	3535 and 3354 cm^{-1}
aliphatic $–CH_2$/$-CH_3$ stretching [17]	2954, 2929 and 2867 cm^{-1}	2958, 2928 and 2868 cm^{-1}	2959, 2928 and 2870 cm^{-1}	2960, 2927 and 2870 cm^{-1}	2960, 2928 and 2871 cm^{-1}
TOH key characteristic peak [14, 15]		1286 cm^{-1}	1291 cm^{-1}		
Carv key characteristic peak [14]	1251 cm^{-1}				1254 cm^{-1}
Carv key characteristic peak [15]	1173 cm^{-1}		1181 cm^{-1}	1177 cm^{-1}	1175 cm^{-1}
TOH meta-substitution [14]		1156 cm^{-1}	1152 cm^{-1}	1143 cm^{-1}	
Carv ortho-substitution [14, 15]	1116 cm^{-1}		1112 cm^{-1}	1115 cm^{-1}	1116 cm^{-1}
TOH key characteristic peak [15]		1096 cm^{-1}	1089 cm^{-1}	1103 cm^{-1}	
TOH1:3:4-substitution [15]					1036 cm^{-1}
Carv 1:2:4-Substituion [14]	994 cm^{-1}		995 cm^{-1}	996 cm^{-1}	995 cm^{-1}
TOH key characteristic peak [14, 15]		943 cm^{-1}	945 cm^{-1}		937 cm^{-1}
Carv key characteristic peak [14]	865 cm^{-1}				864 cm^{-1}
Carv C–H out-of-plane [14]	812 cm^{-1}				813 cm^{-1}
TOH C–H out-of-plane [14, 15]		804 cm^{-1}	808 cm^{-1}		
TOH ring vibrations [15]		740 cm^{-1}	739 cm^{-1}	740 cm^{-1}	

943 cm^{-1} [14,15], 804 cm^{-1} (TOH –CH out of plane vibration) [14, 15] and 740 cm^{-1} (TOH phenolic ring vibration) [15].

3.3.2. Essential oils

ATR-FTIR spectra of essential oils are also included in Figure 3 (C-E, upper panels). *T. vulgaris* (Figure 3C) essential oil reveals –OH stretching bands at (3553 and 3411 cm^{-1}), peaks attributed to aliphatic $–CH_2$/$-CH_3$ stretching at 2959, 2928 and 2870 cm^{-1}, as well as characteristic signals of TOH (1291, 1152, 1089, 945, 808 and 739 cm^{-1}) and Carv (1181, 1112 and 995 cm^{-1}), among others summarized in Table 2.

O. vulgare spectrum (Figure 3D) shows characteristic signals of Carv at 1177, 1115, 996 cm^{-1}, and very low intensity peaks assigned to TOH fingerprints such as 1143, 1103 and 740 cm^{-1}. These results are in agreement with high percentage of Carv (87.6%) and minimal amount of TOH (<0.1%) detected by GC-MS.

The spectrum of *O. X applii* essential oil (Figure 3E) depicts fingerprint peaks of Carv at 1254, 1175, 1116, 995, 937, 864 and 813 cm^{-1} [14,15] and of TOH at 1036 cm^{-1} [15].

3.3.3. ATR-FTIR analysis of layers formed on Pt electrodes

The compositions of the layers formed on the Pt electrodes after the cyclic voltammetry assays were also analyzed by ATR-FTIR and the spectra were included in Figure 3 (A-E, lower panels). The contributions are summarized in the corresponding Table 3.

ATR-FTIR spectrum of Pt surface after potentiodynamic assays with Carv depicts contributions attributed to phenolic rings (1490, 1270, 1152, 1030, 1001, 942, 894, 867, 785, 756, 720 and 700 cm^{-1}) [4–6], isopropyl groups (1454, 1361 and 1342 cm^{-1}), ether bonds (1244, 1180 and 814 cm^{-1}) [4,6] and polysubstituted phenolic rings (3022 and 1397

Table 3. Wavenumbers and assignments (according to literature data) obtained for polymeric layers formed on Pt electrodes after the electrochemical assays made with the organic compounds.

	Pt Carv	Pt TOH	Pt *T. vulgaris*	Pt *O. vulgare*	Pt *O. X applii*
Aliphatic CH_3/CH_2 [17,18]	2960, 2927 and 2869 cm^{-1}	2954, 2921, 2877 and 1328 cm^{-1}	2959, 2916 and 2861 cm^{-1}	2957, 2920 and 2876 cm^{-1}	2953, 2927 and 2866 cm^{-1}
Phenolic ring CH vibrations [17, 18, 19]	1490, 1270, 1152, 1030, 1001, 942, 894, 867, 785, 756, 720 and 700 cm^{-1}	1006, 892, 853, 809 and 743 cm^{-1}	1519, 1237, 891 and 806 cm^{-1}	1025, 1009, 939, 851 and 810 cm^{-1}	1615, 1501, 1488, 1454, 1444, 1023, 890, 856 and 810 cm^{-1}
Ether bonds [17, 19]	1244, 1180 and 814 cm^{-1}	1172, 1112, 1041 and 809 cm^{-1}	1161, 1099, 1032 and 813 cm^{-1}	1173, 1118 and 810 cm^{-1}	1285, 1251, 1173 and 810 cm^{-1}
-C=O [18, 26]			1685 cm^{-1}		1721 and 1677 cm^{-1}

cm^{-1}) [4], evidencing the absence of –OH bands. Carv deposition, oxidation and electropolymerization on metal surface can be inferred.

ATR-FTIR analysis of Pt surface after TOH treatment (Figure 3B) showed bands at 1006, 892, 853, 809 and 743 cm^{-1} (phenolic C–H vibrations) [4, 5, 6], peaks in 2954, 2921, 2877 and 1328 cm^{-1} (deformation and stretching vibration of aliphatic -C-H) [4, 5], at 1217 and 1006 cm^{-1} (Ph-OH), at 1172, 1112, 1041 and 809 cm^{-1} (ether bonds) [4, 6], also indicating TOH oxidation and electropolymerization on the metal surface.

Interestingly, the spectrum of Pt surface with *T. vulgaris* essential oil evidences phenolic structures deposition (-C-H phenolic ring vibrations at 1519, 1237, 891 and 806 cm^{-1}, and $–CH_2/-CH_3$ aliphatic stretching at 2959, 2916 and 2861 cm^{-1} [4,5]), oxidation (1685 cm^{-1}, non hydrogen bonding –C=O) [7], polymerization (ether bonds at 1161, 1099, 1032 and 813 cm^{-1} [4]) and absence of –OH broad band, indicating that the blockage of Pt surface is due to the deposit followed by the electropolymerization of phenolic compounds from essential oil.

On the other hand, the spectrum of Pt surface after *O. vulgare* treatment depicts signals at 1025, 1009, 939, 851 and 810 cm^{-1} attributed to phenolic ring -C-H vibrations [4, 5]; at 2957, 2920 and 2876 cm^{-1} (aliphatic -C-H vibrations) [4]; peaks corresponding to ether bonds at 1233, 1173, 1118 and 810 cm^{-1} [4,5] and a band assigned to –C=O at 1686 cm^{-1}. It is important to notice the absence of hydroxyl bands (3700-3000 cm^{-1}). Thus, spectra indicate the electropolymerization of phenolic compounds of essential oil that remain attached to metal surface.

Spectrum of Pt surface after *O. x applii* treatment shows peaks attributed to –OH and –C=O (ketone) vibrations (3286, 1677, 1721, 1677, 1376 and 1420 cm^{-1}) [5,6,8], to -C-H of phenolic rings (1615, 1501, 1488, 1454, 1444, 1023, 890, 856 and 810 cm^{-1}) [4–6,9], to aliphatic $–CH_2/CH_3$ (2953, 2927 and 2866 cm^{-1}) [4] and to ether bonds (1285, 1251, 1173 and 810 cm^{-1}) [4,5,10,11]. Thus, polymerization or electrodeposition of phenolic compounds can take place on the electrode surface, due to the presence of hydroxyl and ketone signals.

ATR-FTIR analysis indicates that polymeric or electrodeposited phenolic compounds layers that block the metal surface are formed on Pt electrodes after the electrochemical assays with the pure drugs and the essential oils [17, 18, 19, 20, 21].

3.4. Electropolymerization of phenolic compounds on Cu electrodes

Considering that a distinctive behavior for Carv-containing samples could not be found to differentiate Carv from TOH using Pt electrodes, Cu electrodes were employed to investigate if distinguishing and conclusive features could be found.

3.4.1. Pure carvacrol and thymol

Potentiodynamic assays were made with Cu electrodes in order to investigate if this accessible and inexpensive electrode could be used to distinguish the presence of Carv from TOH in essential oils.

Figure 4A shows that in case of pure Carv there is a unique peak at 0.38 V that falls to zero close to the anodic potential limit and remains nil during the following cycles in the whole potential range [22]. After the electrochemical assay, a bright layer was formed on the electrode surface. Instead, a broad peak at 0.46 V and a shoulder at the anodic side were obtained in case of TOH (Figure 4B) and an opaque deposit could be seen after the assay. An additional difference in the TOH response in relation to Carv can be distinguished during the cathodic scan since positive current densities were recorded, indicating that the oxidation of TOH also occurs during this reverse scan. To investigate this topic, mixtures of Carv and TOH were assayed and compared with those of the pure components. Figure 4C shows that the voltammogram of the mixture with different contents of Carv (TOH/Carv = 1/4 and 1/2) denotes the presence of Carv since current density dropped to zero value as it was observed for pure Carv, but a shoulder associated to TOH can be detected at the anodic side of the peak.

Carv layers formed on Cu electrodes are bright and homogeneous at naked eye. AFM images (Figure 5), and the section analysis are according with these characteristics, that is, there are only a few nanometers between valleys and tops. On the other hand, TOH layers are rougher with section analysis that show differences close to 100 nm between the valleys and the tops. The homogeneous layers obtained with Carv are in

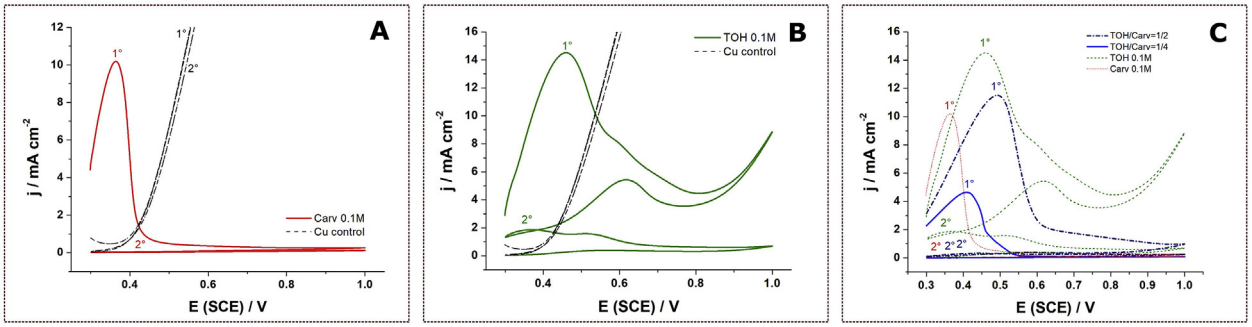

Figure 4. Voltamperometric cycles made at 50 mVs^{-1} with Cu electrodes in A) 0.1 M Carv (red lines), B) 0.1 M TOH (green lines) in hydroalcoholic solution. Dotted lines represent Cu electrode in electrolyte control without phytocompound. C) Comparison between pure drugs and the mixtures: TOH/Carv = 1/4 and TOH/Carv = 1/2.

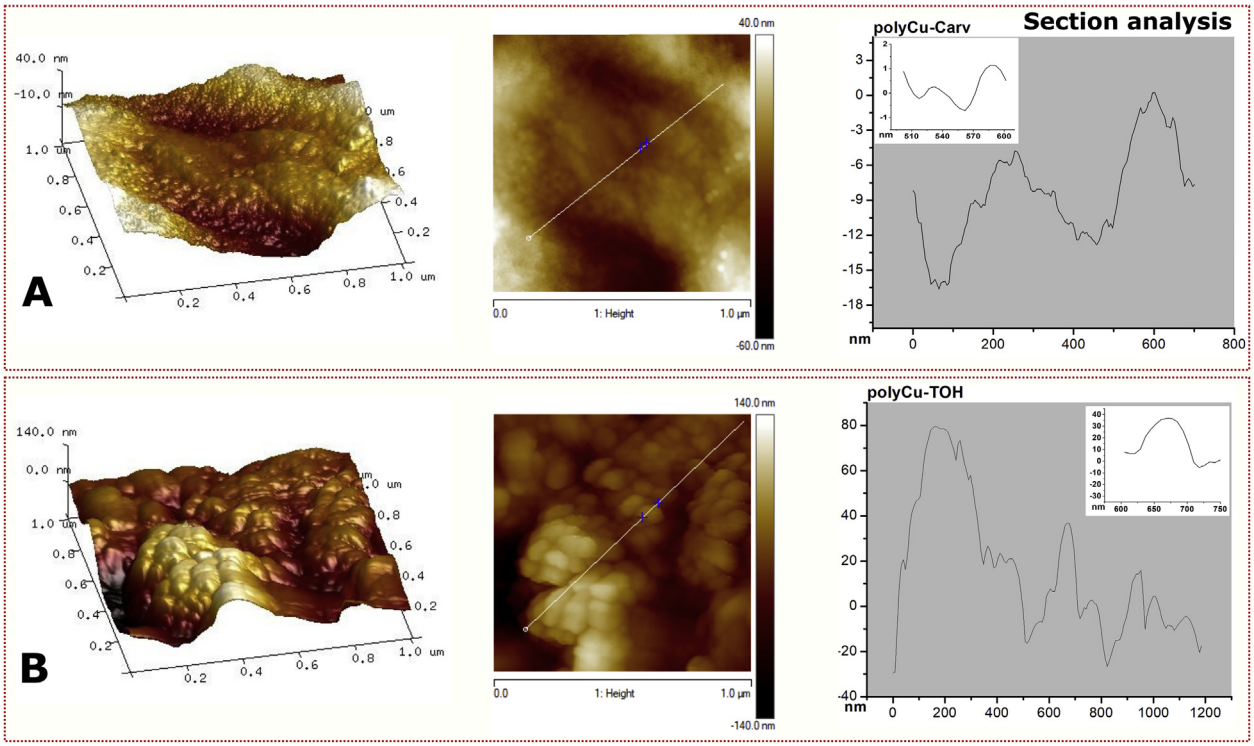

Figure 5. AFM images obtained after potentiodynamic assays made with Cu electrodes with Carv (A) and TOH (B) solutions. The Section analysis on the left corresponds to the records obtained from the section indicated with the lines (center).

agreement with the low current values, close to zero, recorded after the potententiodynamic and potentiostatic records that are related to the presence of the blocking layer. This electrochemical behavior was not observed with TOH, due to the non-homogeneous rough film formed on the Cu surface.

3.4.2. Essential oils

In order to identify Carv in essential oils, voltammograms were recorded with these natural mixtures of phenolic compounds.

In case of *O. vulgare* (Figure 6A) they show two peaks during the first cycle. One of them, close to 0.40 V, drastically decreases to zero during the second cycle. A second peak at 0.70 V was detected and it was lower but significant during the second cycle.

The voltammogram obtained with *O. x applii* (Figure 6B) during the first cycle shows a contribution in the vicinity of 0.40 V which disappears during the second cycle, as observed in case of pure Carv and *O. vulgare*. At higher potentials, there is another broad contribution at 0.60 V that may be associated to TOH and/or other components that are oxidized near the anodic limit of the potentiodynamic record. Additionally, the current density at the anodic limit does not markedly decrease upon cycling as in case of the pure components Carv and TOH. Interestingly, the height of the 0.40 V current peak of the essential oils follows the sequence *O. vulgare* > *O. x applii* > *T. vulgaris* revealing the same order of the content of Carv in the essential oils.

In case of *T. vulgaris* (Figure 6C), current densities in the 0.30 V–0.80 V potential range are lower than in previous cases. It is worthy to note that this oil contains a high level of TOH (78.4%) but low percentage of Carv (2%). The contribution close to 0.40 V is low but it can be seen that it is near zero during the second cycle. Notwithstanding the concentration of TOH is high in this essential oil, its oxidation peak is low and seems to be hindered by the other components of the essential oil.

Therefore, considering the results of Figure 6, the presence of Carv in the essential oils can be identified by analyzing comparatively the first and the second potentiodynamic cycles: if current density recorded in the vicinity of 0.40 V in the first cycle dropped to zero during the second one, this contribution could be attributed to Carv.

To reinforce this hypothesis and taking into account that 0.40 V is close to the peak potential corresponding to the oxidation of pure Carv on Cu, potentiostatic assays at this potential value were made (Figure 7). They showed that when Carv is present, even at low concentration (2% in *T. vulgaris*) current transients decrease to zero within the first 30s. Particularly, current drops to zero after 4 s in case of pure Carv, at 6 s in

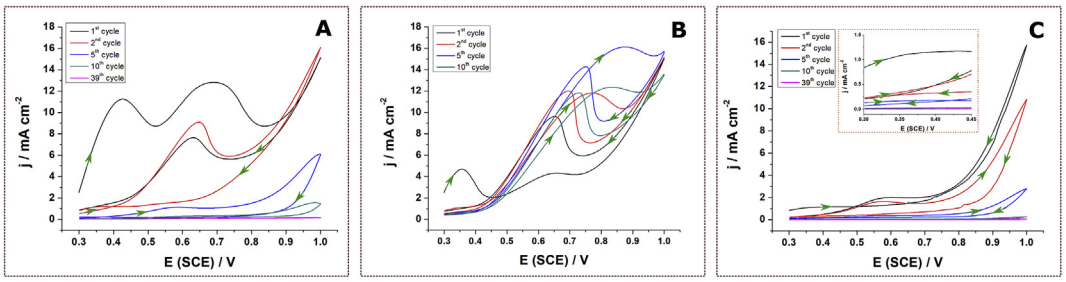

Figure 6. Voltamperometric cycles made at 50 mVs^{-1} with Cu electrodes in A) *O. vulgare*, B) *O. x applii* and C) *T. vulgaris* essential oils in hydroalcoholic solution (inset correspond to record detail in region between 0.30 and 0.45 V).

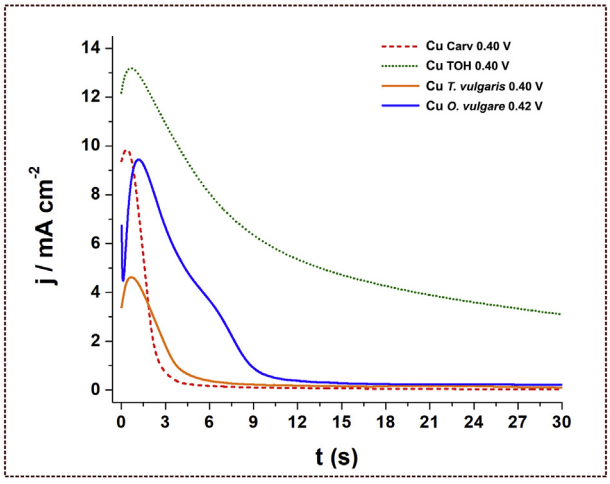

Figure 7. Chronoamperometric records made at 0.40 V with Cu electrodes in Carv, TOH, *T. vulgaris* and *O. vulgare* solutions.

case of *T. vulgaris* (2% Carv), 10 s in case of *O. vulgare* (87.6% Carv) but remain at high values in case of pure TOH.

3.5. ATR-FTIR analysis of the layers formed on Cu electrodes

After the analysis of potentiodynamic and potentiostatic curves the question that arises is: why the current values drop to zero when Cu is used as working electrode in presence of Carv? It was previously mentioned that a thin, bright polymeric film was formed on the electrode in the case of Carv and an opaquer layer in the case of TOH (hereinafter we will call this kind of films polyCu). The ATR-FTIR of polyCu obtained with TOH, Carv, TOH/Carv = 1/2, *O. vulgare* and *T. vulgaris* showed, in agreement with previous reports [17], the signals associated to ether bonds. The layers formed on *O. x applii* were very labile and did not remain attached to the surface.

In Figure 8 and Table 4 the bands related to ether bonds (1247, 1182, 1115 and 1046 cm^{-1}) [19,23–25] and a peak at 1674 cm^{-1} assigned to groups –C=O without hydrogen bridge bonds are reported [17, 18, 26]. Furthermore, the characteristic peaks 3300-3500 cm^{-1} corresponding to –OH groups without hydrogen bridge bonds [26, 27, 28, 29] observed in the pure compounds and mixtures, are not detected in the polyCu.

3.6. Comparative analysis of results obtained with Cu electrodes

All thing considered, when Carv is present, its polymerization occurs at more cathodic potentials than that of TOH. The characteristic current drop associated to the blockage of the electrode active sites and the formation of the brilliant layer on the surface is likely owed to the particular molecular structure of Carv (with OH in the *meta* position respect to isopropyl group that facilitates the dimerization through ether bonds formation followed by polymerization). Instead, TOH is characterized by the OH in the *ortho* position that hinders the formation of dimers and polymerization process on the electrode surface.

3.6.1. Electropolymerization mechanism of Carv containing essential oils

Electrochemical treatments of Cu electrodes in Carv containing solutions lead to the electropolymerization of this phenolic compound according to the following mechanism (adapted from [30]):

$$PhD_{(ac)} \leftrightarrow PhD_{(ad)} \quad (1)$$

$$PhD_{(ad)} + PhD_{(ad)} \leftrightarrow PhD_{2(ad)} + 2e^- + 2H^+_{(ac)} \quad (2)$$

$$PhD_{(ad)} \leftrightarrow PhD^{\circ+}_{(ad)} + e^- \quad (3)$$

$$PhD^{\circ+}_{(ad)} + PhD_{(ad)} \leftrightarrow PhD_{2(ad)} + e^- + 2H^+_{(ac)} \quad (4)$$

$$PhD_{2(ad)} \leftrightarrow PhD^-_{2(ad)} + H^+ \quad (4a)$$

$$PhD^-_{2(ad)} \leftrightarrow PhD_{2(ad)}{}^{\circ} + e^- \quad (4b)$$

where $PhD_{(ad)}$ is an adsorbed molecule of phenolic compound (mainly Carv, due to its molecular structure), $PhD^{\circ+}_{(ad)}$ corresponds to an adsorbed cationic radical and $PhD_{2(ad)}$ is an adsorbed dimer. Initially, PhD single molecules adsorb to the surface and may be oxidized generating adsorbed dimers in one or two steps (Eqs. (1), (2), (3), and (4)). Dimers may lose a proton in alkaline electrolyte (Eq. (4a)) leading the formation of $PhD^-_{2(ad)}$ anions. Subsequently, during polymerization the loss of one electron occurs (Eq. (4b)). Successive oxidations transform dimers to oligomers that could attach to the metallic surface (Eqs. (5) and (6)).

$$PhD_{n(ad)} \leftrightarrow PhD^{\circ+}_{n(ad)} + e^- \quad (5)$$

$$PhD^{\circ+}_{n(ad)} + PhD_{(ad)} \leftrightarrow PhD_{n+1(s)} + e^- + 2H^+_{(ac)} \quad (6)$$

$$PhD_{m(s)} + PhD_{(ac)} \leftrightarrow PhD_{m+1(s)} + 2e^- + 2H^+_{(ac)} \quad (7)$$

The metal surface blockage by the formation of insoluble products attached to the surface as $PhD_{n+1(s)}$ and $PhD_{m+1(s)}$ can be seen in Eqs. (5), (6), and (7), where $PhD^{\circ+}_{n(ad)}$ is an adsorbed radical cation oligomer.

The proposed electropolymerization mechanism of Carv-containing mixtures or essential oils depicts important contributions of Carv dimmers and oligomers adsorbed on the electrode surface that react to produce polymeric insoluble macromolecules, leading to the blockage of the metal surface principally by a smooth Carv polymer. Consequently, this distinctive property should allow to characterize the presence of Carv in the mixtures because the other components such as TOH are not able to form such a brilliant, continuous and blocking layer [17] in this potential region. Thus, unambiguous signals of the presence of Carv in the essential oil when TOH, its positional isomer, is also present can be obtained either using cyclic voltammetry or potentiostatic records. In case of cyclic voltammetry the presence of Carv can be detected through the current contribution close to 0.40 V during the anodic record that decreases to zero during the reverse scan of the first cycle and the following cycles. On the other hand, for potentiostatic assays, the distinctive behavior corresponds to the current drop to zero during the first 30 s in the transient current recorded at this potential.

Additional relevant technological outcomes are related to the polymeric layer formed using Carv-containing essential oils on Cu since they provide important effects: this layer can operate as an eco-friendly corrosion inhibitor and as antimicrobial agent in industrial (Cu piping) and medical applications (intrauterine devices), avoiding the release of Cu ions that impact on the environment and on human health, according to our previous works [17, 31].

4. Conclusions

Results show that Carv can be detected and distinguished from its positional isomer TOH in mixtures and in essential oils using Cu as working electrode by cyclic voltammetry or by potentiostatic records accomplished close to 0.40 V. This simple potentiostatic test could be made with a basic power source and a compiler and may be suitable for the detection in production farms of aromatic plants. The distinctive detection of Carv could be made thanks to its capacity to form a bright polymeric layer that blocks the Cu surface. As a consequence, potentiostatic records close to this potential show a peak and a sharp decrease of current to zero values. On the other hand, potentiodynamic cycles depict a current contribution in the vicinity of 0.40 V and values close to zero during the cathodic scan and the following cycles in this potential region. The formation of ether bonds was involved in the development of the polymeric blocking layers according to FTIR and AFM analysis. Conversely, assays with Pt electrodes were not suitable to identify unambiguously the presence of Carv.

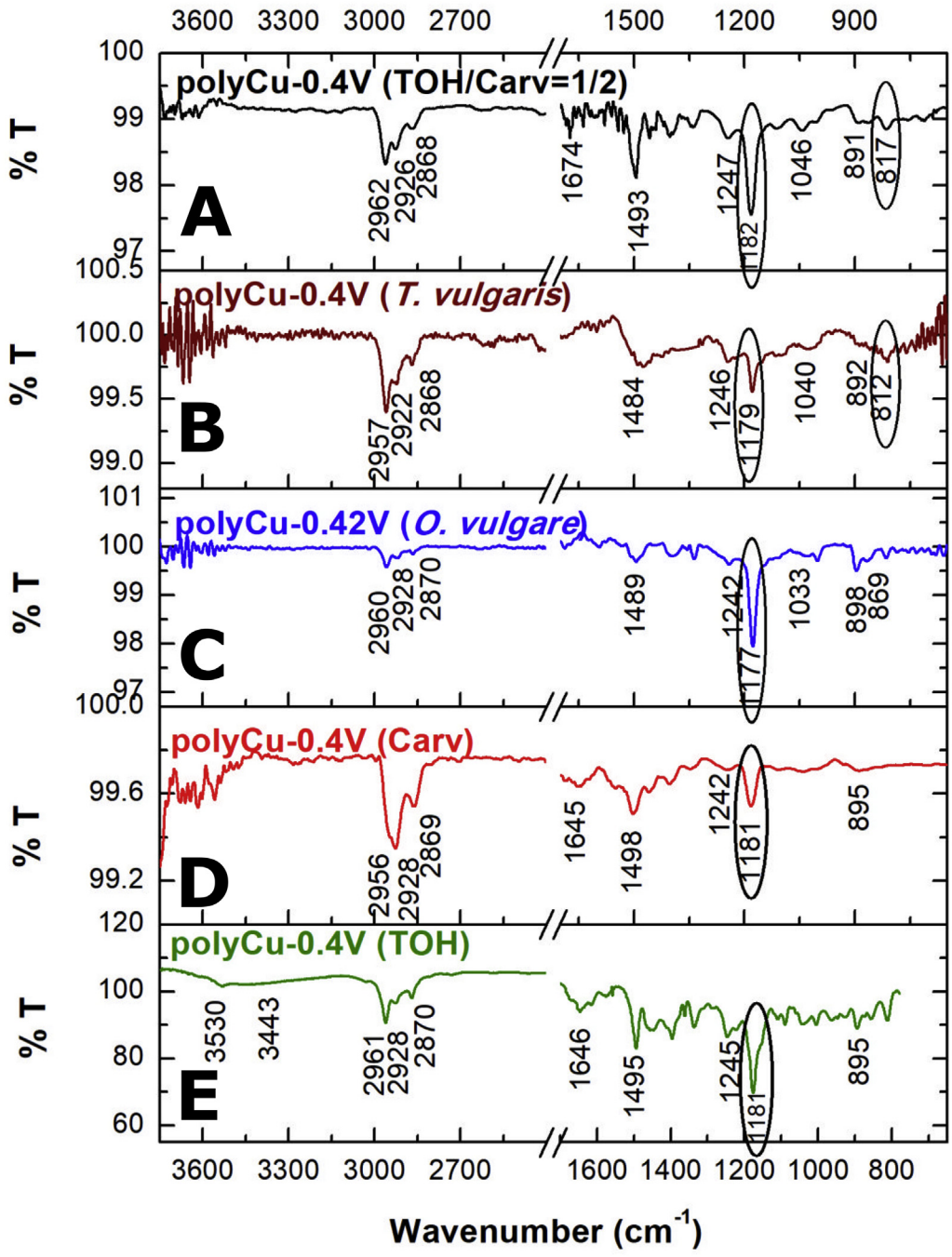

Figure 8. ATR-FTIR spectra obtained for Cu electrodes after the potentiostatic treatments at 0.40 V made with A) TOH/Carv = 1/4 mixture, B) *T. vulgaris*, C) *O. vulgare,* D) Carv and E) TOH.

Electropolymerization mechanism occurred on Cu in presence of Carv-containing essential oils depicts important contributions of Carv dimmers and oligomers adsorbed to the electrode surface that react to produce polymeric insoluble macromolecules attached to Cu. This leads to the formation of a homogeneous and compact Carv polymeric layer on Cu.

Table 4. Wavenumbers and assignments (according to literature data) obtained for polymeric layers formed on Cu electrodes after the potentiostatic assays made with the organic compounds.

	Cu Carv	Cu TOH	Cu TOH/Carv = 1/2	Cu *T. vulgaris*	Cu *O. vulgare*
-OH stretching vibration [17]		3530 and 3443 cm^{-1}			
Aliphatic CH_3/CH_2 [17,18]	2956, 2928 and 2869 cm^{-1}	2961, 2928, 2870 cm^{-1}	2962, 2926 and 2868 cm^{-1}	2957, 2922 and 2868 cm^{-1}	2960, 2928 and 2870 cm^{-1}
Phenolic ring CH vibrations [17, 18, 19]	1498 and 895cm^{-1}	1495 and 895cm^{-1}	1493, 1046 and 891 cm^{-1}	1484, 1040, 892 and 812 cm^{-1}	1489, 898 and 869 cm^{-1}
Ether bonds [17, 19]	1242 and 1181 cm^{-1}	1245 and 1181 cm^{-1}	1247, 1182 and 817 cm^{-1}	1246, 1179 and 812 cm^{-1}	1242, 1177 and 1033 cm^{-1}
-C=O [18, 26]	1645 cm^{-1}		1674 cm^{-1}		

Apart from the detection of Carv, additional technological outcomes related to the polymeric films obtained on Cu with Carv-containing essential oils are worthy to mention: they can be used both, as eco-friendly corrosion inhibitor and as antimicrobial agent in industrial (Cu piping) and medical applications (intrauterine devices), avoiding the environmental impact of Cu ions release and toxic effects on human body and allowing the improvement of their biocompatibility.

Declarations

Author contribution statement

Mónica Fernandez Lorenzo de Mele: Conceived and designed the experiments; Analyzed and interpreted the data; Contributed reagents, materials, analysis tools or data; Wrote the paper.

Marcos Bertuola, Natalia Fagali: Performed the experiments; Analyzed and interpreted the data; Wrote the paper.

Funding statement

This work was supported by CONICET (Grant Number [P-UE22920170100100CO]), UNLP (Grant Number [11/I221]), ANPCyT (Grant Number [PICT2016-1424]).

Competing interest statement

The authors declare no conflict of interest.

Additional information

No additional information is available for this paper.

Acknowledgement

Authors would like to acknowledge Esther Svartman for her kind assistance in CG-MS measurements.

References

[1] M. Sharifi-Rad, E.M. Varoni, M. Iriti, M. Martorell, W.N. Setzer, M. del Mar Contreras, B. Salehi, A. Soltani-Nejad, S. Rajabi, M. Tajbakhsh, J. Sharifi-Rad, Carvacrol and human health: a comprehensive review, Phytother Res. 32 (2018) 1675–1687.

[2] A. El Jaouhari, S. Ben Jadi, Z. Aouzal, M. Bouabdallaoui, E.A. Bazzaoui, R. Wang, M. Bazzaoui, Comparison study between corrosion protection of polypyrrole synthesized on stainless steel from phthalate and saccharinate aqueous medium, Polym. Test. 67 (2018) 302–308.

[3] M. Michalska-Sionkowska, M. Walczak, A. Sionkowska, Antimicrobial activity of collagen material with thymol addition for potential application as wound dressing, Polym. Test. 63 (2017) 360–366.

[4] A. Durazzo, M. Lucarini, E.B. Souto, C. Cicala, E. Caiazzo, A.A. Izzo, E. Novellino, A. Santini, Polyphenols: a concise overview on the chemistry, occurrence, and human health, Phytother Res. 33 (2019) 2221–2243.

[5] J. Xu, F. Zhou, B.P. Ji, R.S. Pei, N. Xu, The antibacterial mechanism of carvacrol and thymol against *Escherichia coli*, Lett. Appl. Microbiol. 47 (2008) 174–179.

[6] A. Alavinezhad, M.R. Khazdair, M.H. Boskabady, Possible therapeutic effect of carvacrol on asthmatic patients: a randomized, double blind, placebo-controlled, Phase II clinical trial, Phytother Res. 32 (2018) 151–159.

[7] F.C. Fachini-Queiroz, R. Kummer, C.F. Estevão-Silva, M.D.D.B. Carvalho, J.M. Cunha, R. Grespan, C.A. Bersani-Amado, R.K.N. Cuman, Effects of thymol and carvacrol, constituents of *Thymus vulgaris* L. essential oil, on the inflammatory response, Evidence-Based Complement, Alternative Med. 2012 (2012) 1–10.

[8] M. Bertuola, C.A. Grillo, M. Fernández Lorenzo de Mele, Eradication of burst release of copper ions from copper-bearing IUDs by a phytocompound-based electropolymeric coating, Mater. Lett. 252 (2019) 317–320.

[9] E. De Falco, E. Mancini, G. Roscigno, E. Mignola, O. Taglialatela-Scafati, F. Senatore, Chemical composition and biological activity of essential oils of *Origanum vulgare* L. subsp. *vulgare* L. under different growth conditions, Molecules 18 (2013) 14948–14960.

[10] A. Guenbour, A. Kacemi, A. Benbachir, L. Aries, Electropolymerization of 2-aminophenol. Electrochemical and spectroscopic studies, Prog. Org. Coating 38 (2000) 121–126.

[11] Z. Ezerskis, Z. Jusys, Electropolymerization of chlorinated phenols on a Pt electrode in alkaline solution Part I : a cyclic voltammetry study, J. Appl. Electrochem. (2001) 1117–1124.

[12] S.M. Sayyah, S.S. Abd-Elrehim, R.E. Azooz, F. Mohamed, Electrochemical study of the copolymer formation between o-chlorophenol and o-hydroxyphenol, J. Kor. Chem. Soc. 58 (2014) 289–296.

[13] H. Nady, M.M. El-Rabiei, G.M.A. El-Hafez, Electrochemical oxidation behavior of some hazardous phenolic compounds in acidic solution, Egypt, J. Petrol. (2016) 669–678.

[14] A.C.S. Valderrama, C. Rojas de Gante, Traceability of active compounds of essential oils in antimicrobial food packaging using a chemometric method by ATR-FTIR, Am. J. Anal. Chem. 8 (2017) 726–741.

[15] H. Schulz, R. Quilitzsch, H. Krüger, Rapid evaluation and quantitative analysis of thyme, origano and chamomile essential oils by ATR-IR and NIR spectroscopy, J. Mol. Struct. 661–662 (2003) 299–306.

[16] I.S. Al-Sheibany, Qualitative and quantitative evaluation of some organic compounds in Iraqi thyme, Natl. J. Chembiosis 19 (2005) 366–379.

[17] M. Bertuola, C.A. Grillo, D.E. Pissinis, E.D. Prieto, M. Fernández Lorenzo de Mele, Is the biocompatibility of copper with polymerized natural coating dependent on the potential selected for the electropolymerization process? Colloids Surf. B Biointerfaces 159 (2017).

[18] Sadtler Research Laboratories, W.W. Simons, The Sadtler Handbook of Infrared Spectra, W.W. Simons, Heyden and Son, Philadelphia, 1978.

[19] I. Poljanšek, M. Krajnc, Characterization of phenol-formaldehyde prepolymer resins by in line FT-IR spectroscopy, Acta Chim. Slov. 52 (2005) 238–244.

[20] G. Nikolic, S. Zlatkovic, M. Cakic, S. Cakic, C. Lacnjevac, Z. Rajic, Fast fourier transform IR characterization of epoxy GY systems crosslinked with aliphatic and cycloaliphatic EH polyamine adducts, Sensors 10 (2010) 684–696.

[21] H.X. Nguyen, H. Ishida, Molecular analysis of the melting behaviour of poly(aryl-ether-ether-ketone), Polymer (Guildf) 27 (1986) 1400–1405.

[22] M. Ferreira, H. Varela, R.M. Torresi, G. Tremiliosi-Filho, Electrode passivation caused by polymerization of different phenolic compounds, Electrochim. Acta 52 (2006) 434–442.

[23] L. Guo, H. Sato, T. Hashimoto, Y. Ozaki, FTIR study on hydrogen-bonding interactions in biodegradable polymer blends of poly(3-hydroxybutyrate) and poly(4-vinylphenol), Macromolecules 43 (2010) 3897–3902.

[24] A.G. Al Lafi, FTIR spectroscopic analysis of ion irradiated poly (ether ether ketone), Polym. Degrad. Stabil. 105 (2014) 122–133.

[25] M. Gattrell, D.W. Kirk, A fourier transform infrared spectroscopy study of the passive film produced during aqueous acidic phenol electro-oxidation, J. Electrochem. Soc. 139 (1992) 2736–2744.

[26] S. Kuo, S. Chan, F. Chang, Miscibility enhancement on the immiscible binary blend of poly (vinyl acetate) and poly (vinyl pyrrolidone) with bisphenol A, Polymer (Guildf) 43 (2002) 3653–3660.

[27] H. Bourara, S. Hadjout, Z. Benabdelghani, A. Etxeberria, Miscibility and hydrogen bonding in blends of poly(4-vinylphenol)/Poly(vinyl methyl ketone), Polymers (Basel) 6 (2014) 2752–2763.

[28] S.W. Kuo, Hydrogen-bonding in polymer blends, J. Polym. Res. 15 (2008) 459–486.

[29] Y.J. Kim, K. Shibata, H. Uyama, S. Kobayashi, Synthesis of ultrahigh molecular weight phenolic polymers by enzymatic polymerization in the presence of amphiphilic triblock copolymer in water, Polymer (Guildf) 49 (2008) 4791–4795.

[30] M. Bertuola, D.E. Pissinis, A.A. Rubert, E.D. Prieto, M.A. Fernández Lorenzo de Mele, Impact of molecular structure of two natural phenolic isomers on the protective characteristics of electropolymerized nanolayers formed on copper, Electrochim. Acta 215 (2016).

[31] M. Bertuola, C.A. Grillo, M.A. Fernández Lorenzo, Reduction of copper ions release by a novel ecofriendly electropolymerized nanolayer obtained from a natural compound (carvacrol), J. Hazard Mater. 313 (2016) 262–271.